**Appendix** for

**Infection with the dengue RNA virus activates TLR9 signaling in human dendritic cells**

Jenn-Haung Lai[a,b,*], Mei-Yi Wang[a], Chuan-Yueh Huang[c], Chien-Hsiang Wu[a], Li-Feng Hung[c], Chia-Ying Yang[a], Po-Yuan Ke[d], Shue-Fen Luo[a], Shih-Jen Liu[e], Ling-Jun Ho[c,*]

**Table of Content**

**Appendix Table S1** qPCR primers and siRNA duplex sequences used in the study

| Gene | Primer Sequence | Gene | Primer Sequence |
|---|---|---|---|
| ***TLR9***<br>NM_017442.3 | F:5'-ACTTCTTCCAAGGCCTGAGC-3'<br>R:5'-GGCCAGGTAATTGTCACGGA-3' | ***TFAM***<br>NM_003201.2 | F:5'-AACCAAAAAGACCTCGTTCAGC-3'<br>R:5'-TTCAGCTTTTCCTGCGGTGA-3' |
| ***IFN-λ1 (IFNL1)***<br>NM_172140.1 | F:5'-GAGGCCCCCAAAAAGGAGTC-3'<br>R:5'-AGGTTCCCATCGGCCACATA-3' | ***mtDNA-2 (mitochondrion)***<br>KY399206.1 | F:5'-TAACCCAAGTCAATAGAAGCC-3'<br>R:5'-CTAGAGGGATATGAAGCACC-3' |
| ***IFN-λ2 (IFNL2)***<br>NM_172138.1 | F:5'-AATTGTGTTGCCAGTGGGGA-3'<br>R:5'-GCGACTGGGTGGCAATAAAT-3' | ***mtDNA-ND1-1 (mitochondrion)***<br>KY399206.1 | F:5'-CCTAGCCGTTTACTCAATCCT-3'<br>R:5'-TGATGGCTAGGGTGACTTCAT-3' |
| ***IFN-λ3 (IFNL2)***<br>NM_172139.3 | F:5'-CCCTGGGGGATGTCTTGGA-3'<br>R:5'-GAGCCAGGGGACTCCTTTTT-3' | ***mtDNA-ND5 (mitochondrion)***<br>KY399206.1 | F:5'-TTCATCCCTGTAGCATTGTTCG-3'<br>R:5'-GTTGGAATAGGTTGTTAGCGGTA-3' |
| ***IFN-β1 (IFNB1)***<br>NM_002176.3 | F:5'-CGCCGCATTGACCATCTA-3'<br>R:5'-GACATTAGCCAGGAGGTTCTCA-3' | ***GAPDH for nDNA***<br>NM_001289746.1 | F:5'-CAATGACCCCTTCATTGACC-3'<br>R:5'-TGGAAGATGGTGATGGGATT-3' |
| ***DENV2***<br>KY586699.1 | F:5'-CTCTCAGTGAACTGCCGGAGACC-3'<br>R:5'-CGTACCATAGGAGGATGCTAGCCG-3' | ***GAPDH for cDNA***<br>NM_001289746.1 | F:5'-AGGTGAAGGTCGGAGTCAAC-3'<br>R:5'-CCATGTAGTTGAGGTCAATGAAGG-3' |
| ***DNase Ⅱ***<br>NM_001375.2 | F:5'-CTCTCAGTGAACTGCCGGAGACC-3'<br>R:5'-CAGCCGGAGTACAGGTCATC-3' | ***siTLR9*** | TLR9-1:5'-GGUGACCGUGCAGCCGGAGAUGUUU-3'<br>TLR9-2:5'-UGGAAGUCCUCGACCUGGCAGGAAA-3'<br>TLR9-3:5'-CCCUGGCGAGUGCCCUGCAAAUACU-3' |
| ***CCR7***<br>NM_001301718.1 | F:5'-GGTGGTGGCTCTCCTTGTCATT-3'<br>R:5'-TGTCTCCGATGTAATCGTCCGTGA-3 | ***siDNaseII (DNASE2)*** | DNaseⅡ-1:5'-CCAGGAAGCCCAGCAGAGCUUAUAA-3'<br>DNaseⅡ-2:5'-GGCUGGUCCACAGUGUACCUAACUU-3'<br>DNaseⅡ-3:5'-GGCAGGUUCUGAAUGUGAACCAGAU-3' |
| ***FLAG*** | F:5'-GAAAAGTGCCACCTGACGC-3'<br>R:5'-GCCCCCGATTTAGAGCTTGA-3' | ***sicGAS (MB21D1)*** | *cGAS*-1:5'-UCAAGACAGUCAGUGGGACCGCAAA-3'<br>*cGAS*-2:5'-AGUUGAAGCUCAGCCGCGAUGAUAU-3'<br>*cGAS*-3:5'-GCACGUGAAGAUUUCUGCACCUAAU-3' |
| ***cGAS***<br>NM_138441.2 | F:5'-AAGAAGAGAAATGTTGCAGGAAAG-3'<br>R:5'-GACTGTCTTGAGGGTTCTGGG-3 | | |
| ***Tlr9 (mouse)***<br>NM_031178.2 | F:5'-GAATCCTCCATCTCCCAACAT-3'<br>R:5'-CCAGAGTCTCAGCCAGCACT-3' | ***Ifnb1 (mouse)***<br>NM_010510.1 | F:5'-AAGAGTTACACTGCCTTTGCCATC-3'<br>R:5'-CACTGTCTGCTGGTGGAGTTCATC-3' |

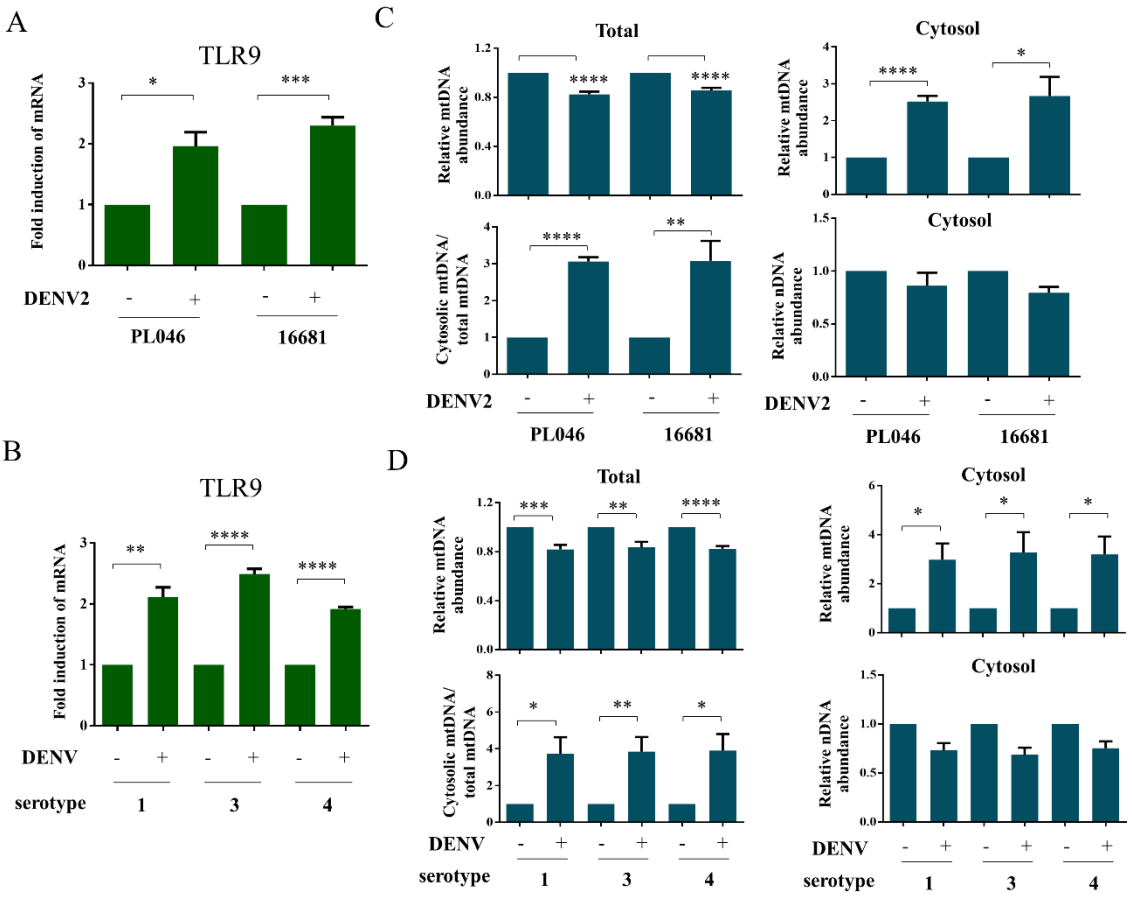


**Appendix figure S1: TLR9 induction and mtDNA release in DCs infected with the four DENV serotypes.**

Human DCs ($1 \times 10^6$ cells/ml) were infected by mock or different strains of DENV at MOI 5 for 24 h. The induction of TLR9 mRNA by DENV serotype 2, including 16681 and PL046 strains (A, n=3), and serotypes 1, 3 and 4 (B, n=3) was analyzed with RT-qPCR. The mtDNA release was also measured (C and D, n=3 for each). Values are means of individual measurements in each sample ± SEM. *P < 0.05, **P < 0.01, ***P < 0.001 and ****P < 0.0001 (unpaired, two-tailed Student's *t*-test).

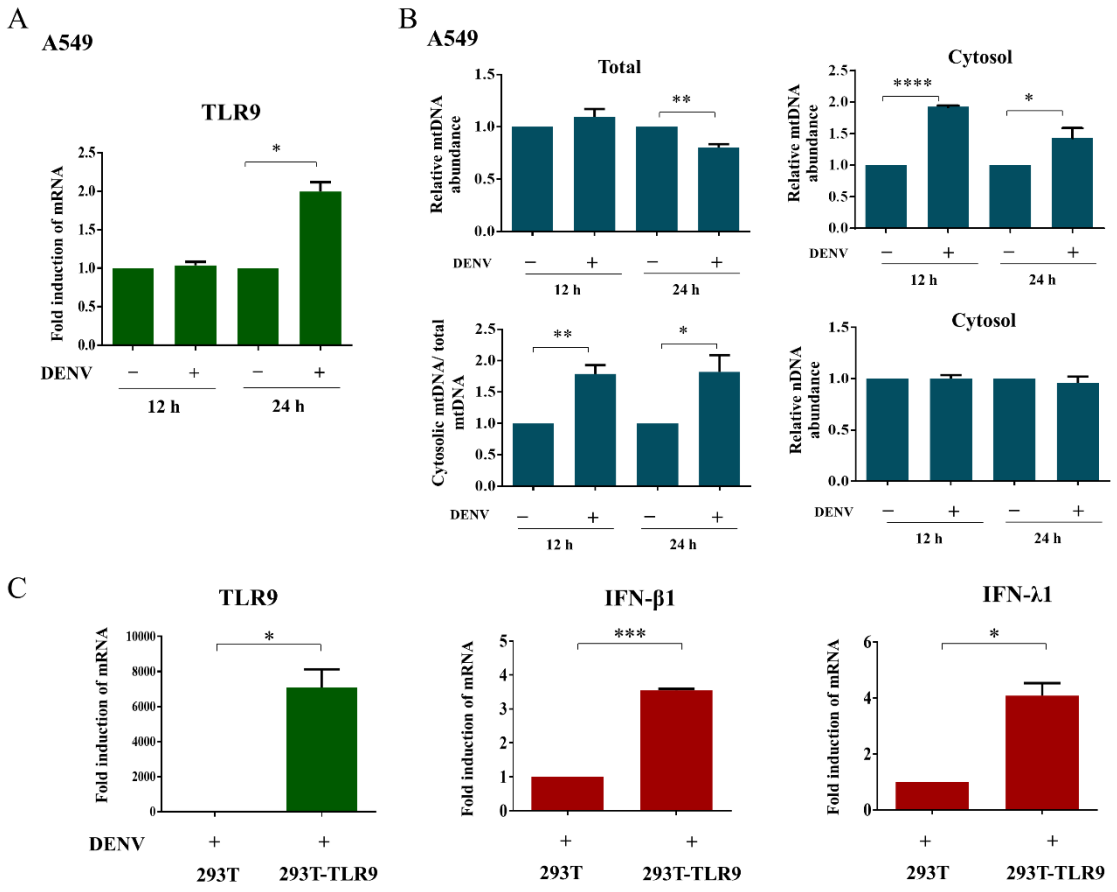


**Appendix figure S2: DENV infection induced TLR9 expression and mtDNA release in A549 cells and the effects of TLR9 in 293T cells.**

The human lung epithelial cell line A549 was examined via experiments similar to those described in Fig. 3B. DENV-induced TLR9 expression (A, n=3) and mtDNA release (B, n=3) were determined. Furthermore, the mRNA levels of TLR9, IFN-β and IFN-λ1 in DENV infected 293T and 293T-TLR9 cells were compared (C, n=3). Values are means of individual measurements in each sample ± SEM. *P < 0.05, **P < 0.01, ***P < 0.001 and ****P < 0.0001 (unpaired, two-tailed Student's *t*-test).

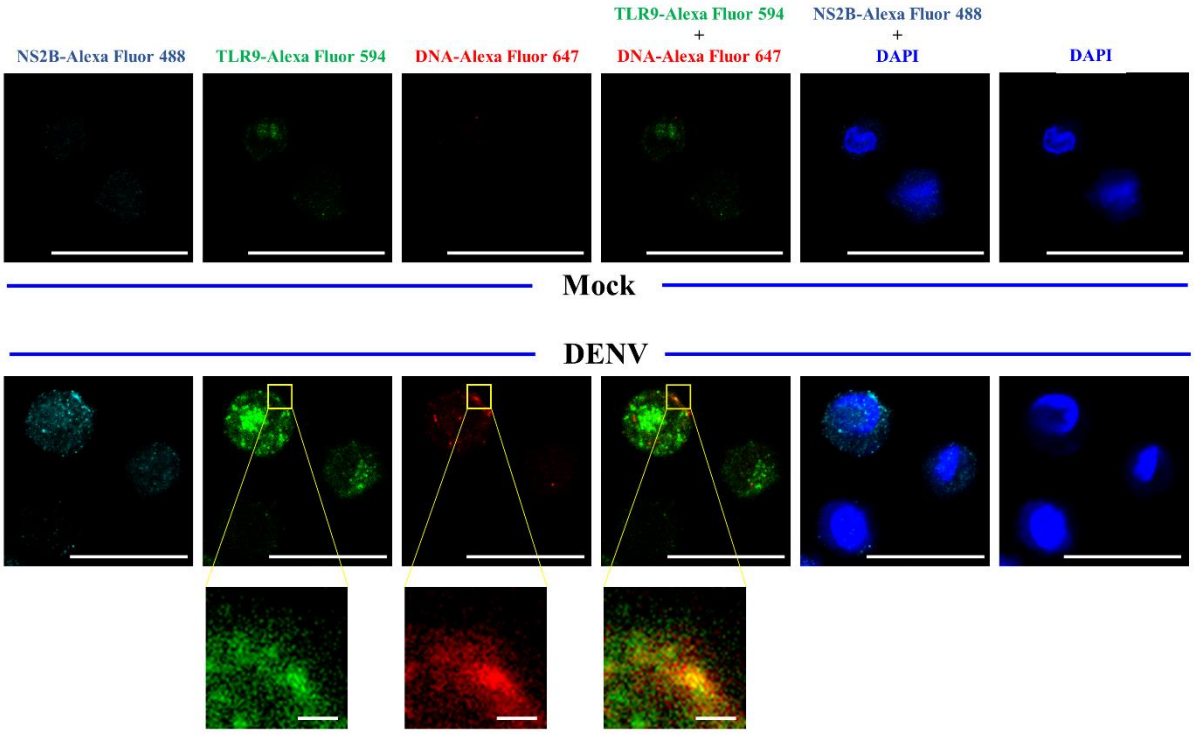


**Appendix figure S3: The colocalization of both TLR9 and DNA in DENV-infected DCs.** Human DCs infected with mock or DENV for 16 h were immunostained with anti-TLR9, anti-NS2B, and anti-DNA antibodies and then counter stained with DAPI. The colocalization of TLR9 and DNA (likely mtDNA) was zoomed. A representative figure from three independent experiments was shown. Scale bar = 20 μm (1 μm in zoomed pictures).

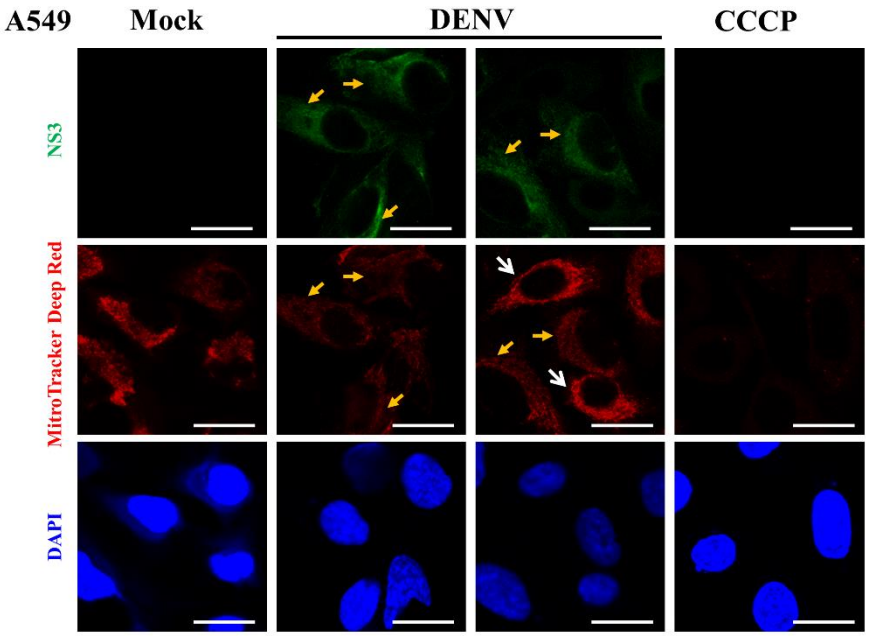


**Appendix figure S4: The intensity of MitoTracker Deep Red signal in A549 cells infected by mock or DENV or treated with CCCP.**

The human lung epithelial cell line A549 cells were infected with mock or DENV for 16 h or treated with CpG (0.5 μM) for 2 h and immunostained with anti-NS3 antibodies and MitoTracker Deep Red and then counter stained with DAPI. In cells that expressed strong signal of MitoTracker Deep Red were stained negative for NS3 (white arrows); in contrast, the NS3-positive cells showed dim intensity of MitoTracker Deep Red signal (yellow arrows). A representative figure from three independent experiments was shown. Scale bar = 20 μm.

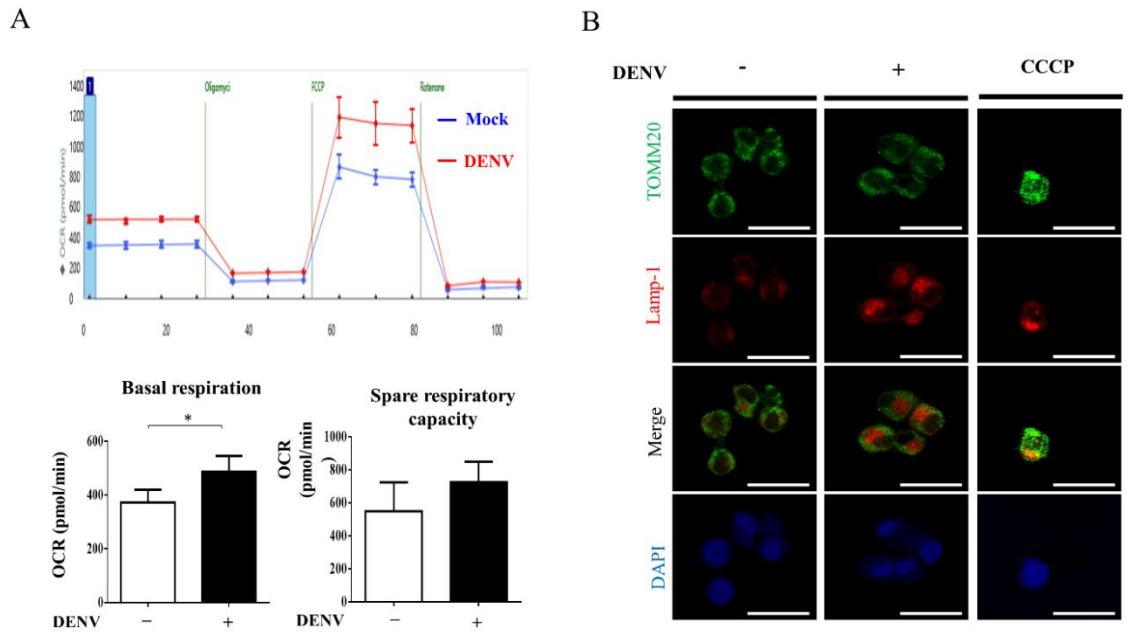


**Appendix figure S5: DENV infection neither affected mitochondrial oxygen consumption nor induced mitophagy in human DCs.**

Human DCs suspended in 100 µl of medium (RPMI with 2% FBS with no $NaHCO_3$) were seeded on Cell-Tak plates pre-coated with Cell and Tissue Adhesive (Corning #354240). After 30 min at room temperature for cell adherence, each well was refilled with 575 µl of medium and was then ready for OCAR evaluation. The OCR was measured with a Seahorse XFe24 metabolic analyzer (Seahorse Bioscience Inc. MA, USA) with an XFe24 FluxPak probe, 102340-00, according to the manufacturer's protocol (A, upper panel). Both basal respiration and spare respiration capacity determined in three different donor cells are shown (A, lower panel, n=3). The presence of mitophagy was monitored by confocal microscope following immunostaining with TOMM20 and Lamp-1 antibodies (B, n=3). Values are means of individual measurements in each sample ± SEM. *P < 0.05 (unpaired, two-tailed Student's *t*-test). Scale bar = 20 µm.

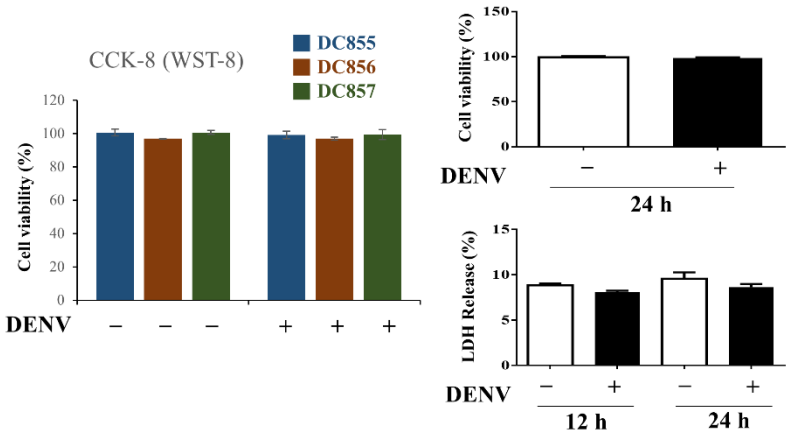


**Appendix figure S6: DENV infection did not increase cell death compared to that in mock infection.**

Human DCs were infected with mock or DENV for 12 h or 24 h and both cells and the culture supernatants were collected for the measurement of CCK-8 (n=3) and LDH release (n=4), respectively according to the experimental procedures. Values are means of individual measurements in each sample ± SEM.

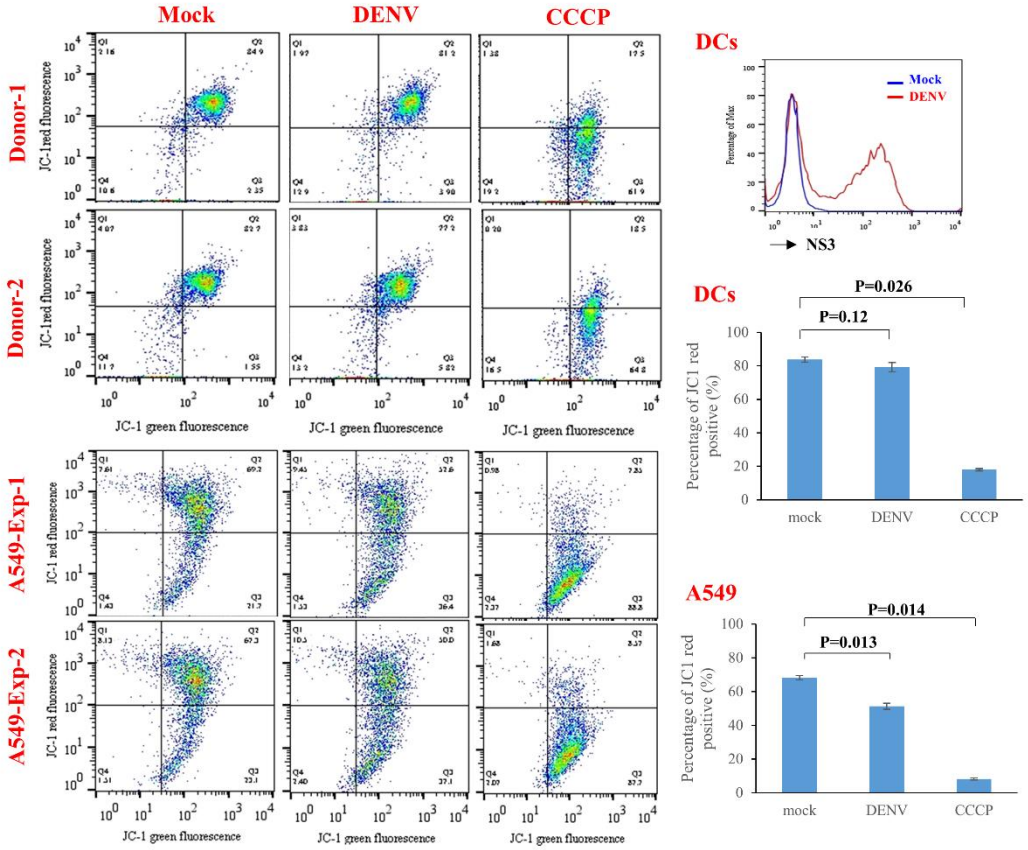


**Appendix figure S7: Changes of mitochondrial membrane potential of DCs and A549 cells in response to DENV infection examined with JC-1 fluorescence probe.**

The human lung epithelial cell line A549 cells or DCs were infected by DENV or mock for 24 h and the cells were stained with both JC-1 red fluorescence and JC-1 green fluorescence as described in experimental procedures and the cells were analyzed under flow cytometry. The data shown were from two different donor DCs and two independent experiments on A549 cells. Values are means of individual measurements in each sample ± SEM. The P values are indicated (unpaired, two-tailed Student's *t*-test analysis).

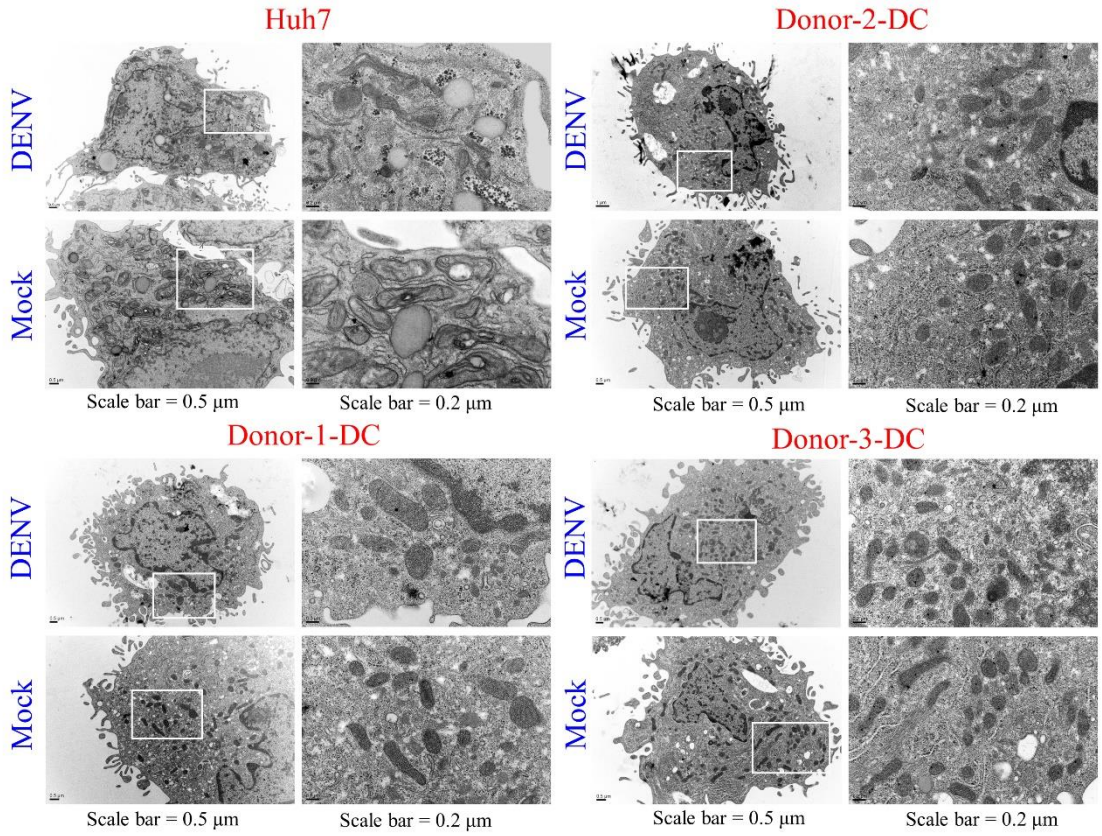


**Appendix figure S8. Pictures of mitochondria in DCs or Huh7 hepatoma cells infected by mock or DENV under transmission electron microscopy (TEM) examination.**

Human DCs or Huh7 cells were infected by mock or DENV (MOI=5) for 8 h and the cells were analyzed under transmission electron microscopy. As the pictures showed, compared to mock infection, there were evident patterns of fusion mitochondria and autophagic vacuoles containing engulfed mitochondria in DENV-infected Huh7 cell. However, there appeared no marked difference in mitochondrial membrane and morphology in DENV-infected DCs compared to those infected by mock. The pictures are representative of 5-6 fields for each group (n=4).

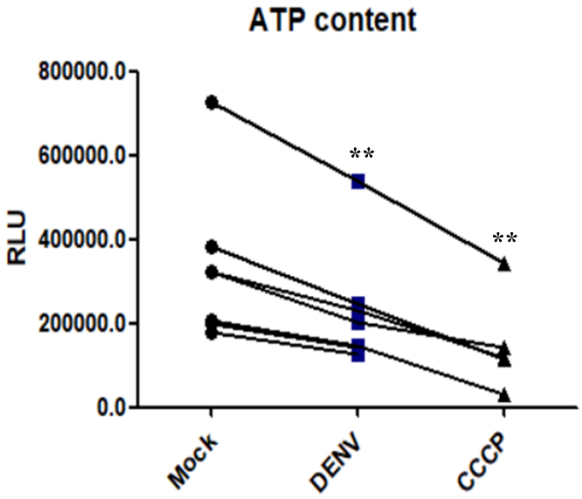


**Appendix figure S9: DENV infection reduced the ATP level in DCs.**

Human DCs ($2 \times 10^4$) were infected with mock or DENV for 24 h or treated with 25 μM CCCP for 1 h. Then, DCs were suspended in 100 μL of culture medium and loaded into opaque-walled 96-well plates. After 100 μL of CellTiter-Glo® luminescent cell viability assay buffer (Promega) was added to each well, and further incubation at room temperature for 10 min, the luminescence intensity was determined by Synergy HT Multi-Mode Microplate Reader (Bio-Tek, Winooski, Vermont, USA). The relative luminescence units (RLU) representing the levels of ATP were measured (n=3). Values are means of individual measurements in each sample ± SEM. **P < 0.01 (unpaired, two-tailed Student's *t*-test).

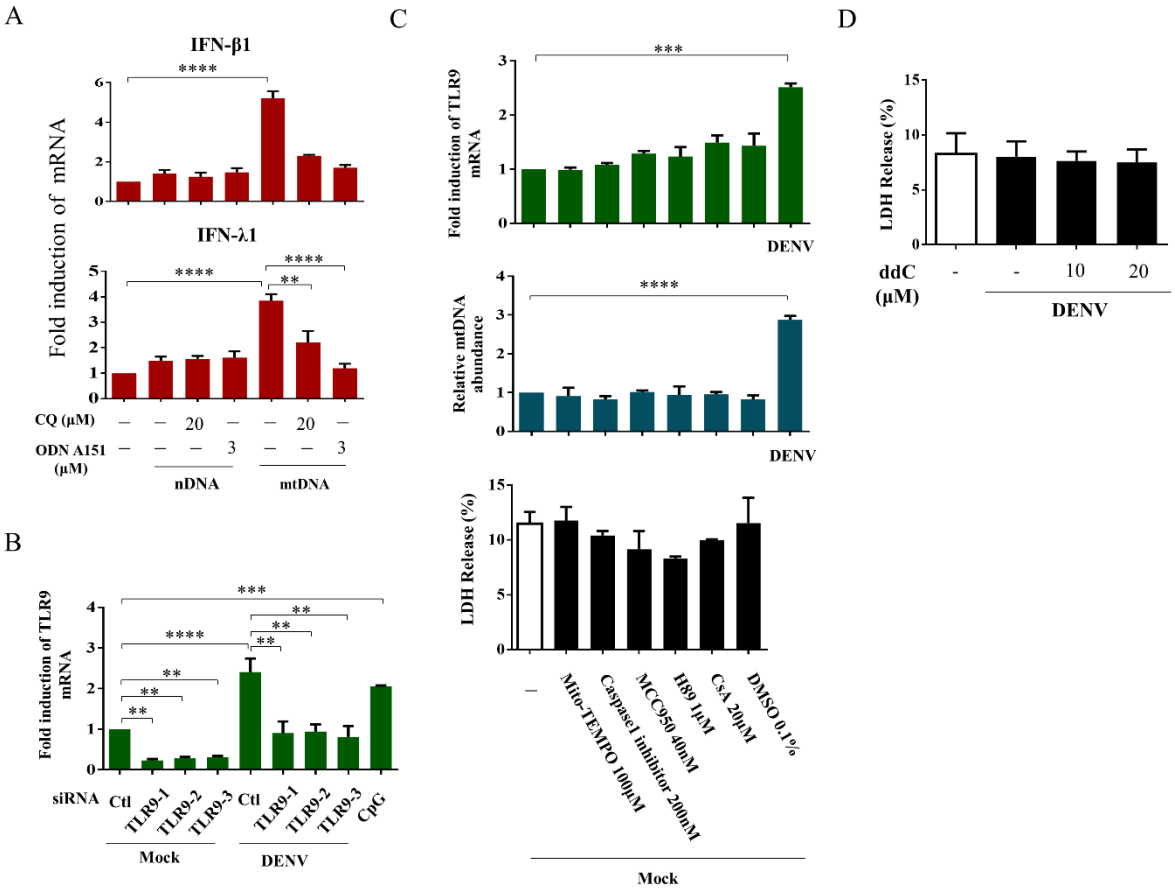


**Appendix figure S10: The potential toxicity of compounds and effects of TLR9 knockdown and compounds on mock-infected or mtDNA-stimulated cells.**

Human DCs were treated with CQ (20 μM) or ODN 151 (3 μM) 30 min before delivery of 1 μg nDNA or mtDNA and IFN-β1 and IFN-λ1 mRNA expression was determined (A, n=3). The effects of TLR9 knockdown in mock- and DENV-infected DCs were determined where CpG treatment was used as a positive control (B, n=3). The effects of various compounds examined in this study on mock-mediated TLR9 mRNA, relative mtDNA abundance (normalized to exogenously added FLAG gene) and LDH release were measured (C, n=2). DENV infection was used as a positive control. The possible cytotoxicity of ddC were determined (D, n=4). Values are means of individual measurements in each sample ± SEM. $^{**}P < 0.01$, $^{***}P < 0.001$ and $^{****}P < 0.0001$ (one-way ANOVA multiple comparisons with Bonferroni post hoc test).

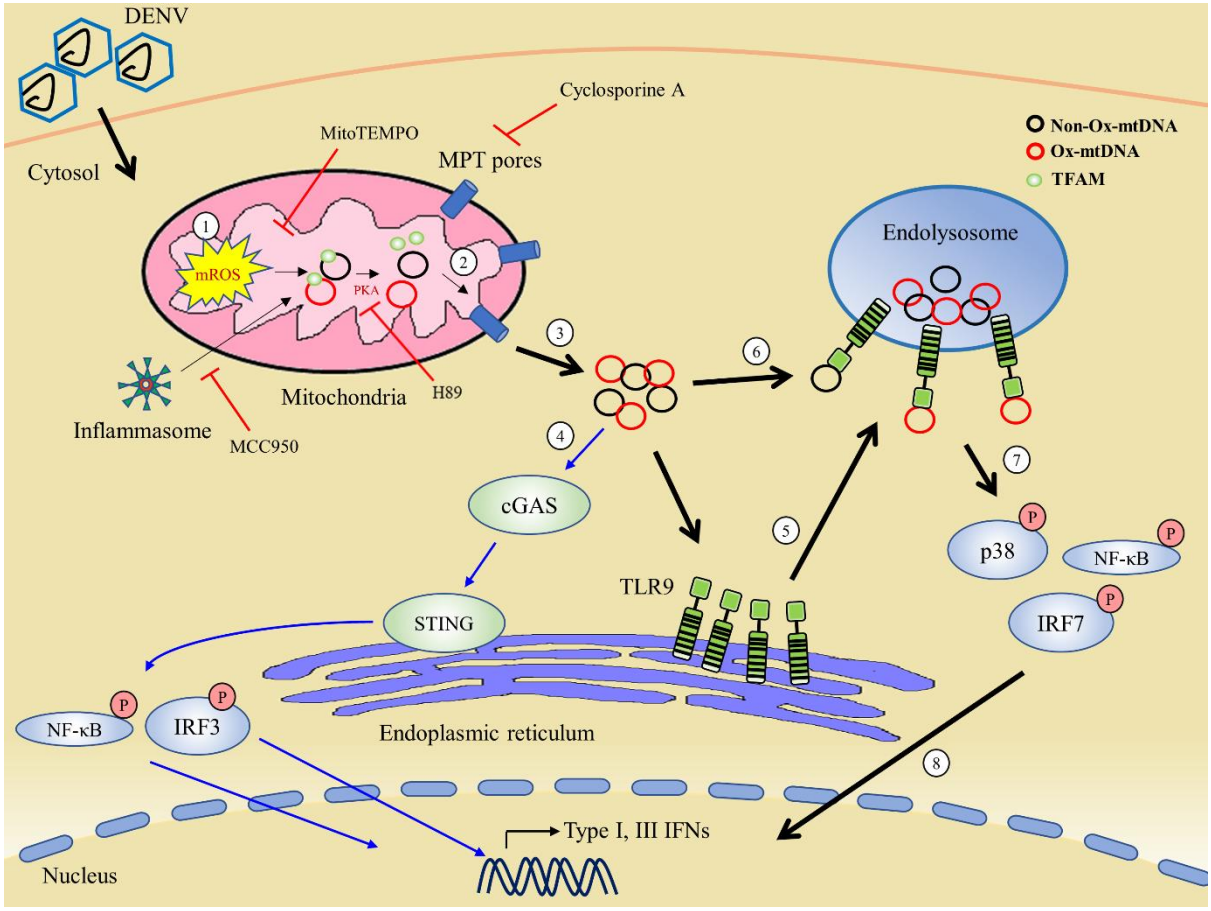


**Appendix figure S11: Schematic diagram of DENV infection-induced mtDNA-TLR9 signaling.**

Infection of human DCs with DENV induces ROS generation and inflammasome activation (1). These events can be inhibited by MitoTEMPO or MCC950 (an inhibitor of NLRP3) treatment. Induction and activation of ROS leads to oxidization of mtDNA, opening of the mitochondrial permeability transition (MPT) pores and release of both non-oxidized and oxidized mtDNA through the MPT pores (2) into the cytosol (3). Cytosolic mtDNA also activates GMP-AMP synthase (cGAS) and stimulator of interferon genes (STING), which engage to activate interferon regulatory factor 3 (IRF3) and NF-κB. In addition, cytosolic mtDNA can induce more TLR9 expression (5) and bind to TLR9 and translocate to

endolysosomes (6). Subsequently, the binding of mtDNA to TLR9 results in phosphorylation and activation of downstream molecules, such as p38, NF-κB and IRF7 (7), and finally leads to the production of IFNs (8).